Engineering Notes

ENGINEERING NOTES are short manuscripts describing new developments or important results of a preliminary nature. These Notes cannot exceed 6 manuscript pages and 3 figures; a page of text may be substituted for a figure and vice versa. After informal review by the editors, they may be published within a few months of the date of receipt. Style requirements are the same as for regular contributions (see inside back cover).

AIAA 81-4075

Electrostatic Potential of an Equatorial Satellite

Nellore S. Venkataraman*
Instituto de Pesquisas Espaciais
Conselho Nacional de Desenvolvimento Científico e Tecnológico—CNPq
São Jose dos Campos, São Paulo, Brasil

Introduction

A SATELLITE moving in the ionosphere builds up a charge because of the differential rate of impingement of electrons and ions. The determination of the electrostatic potential is of importance for determining the electromagnetic forces and torques on the satellite, for wake structure studies, and for correct interpretation of results by on-board instruments. Under steady conditions, a conducting satellite becomes an equipotential if the magnetic field of the Earth is neglected. In the presence of the Earth's magnetic field, because of the induced $V \times B$ field, the satellite will no longer be an equipotential. The determination of the satellite potential and the associated problems have been discussed by a number of authors.[1-5] The effect of geomagnetic substorms and secondary emission of electrons are discussed in Refs. 3 and 4, to which reference can be made for a complete description. The object of this Note is to determine analytically the surface electrostatic potential of a low-altitude spherical satellite of radius R, moving with a constant velocity V, perpendicular to a constant magnetic field B, including the effect of ion thermal motion, photoelectric effect, and the increase in the collection area for ions due to satellite potential.

Estimation of the Satellite Potential

The geometry of the satellite is shown in Fig. 1. The potential on the satellite is determined by the condition that, for equilibrium, the electron current to the satellite (I_e) should be equal to the sum of the ion current (I_i) and the photoelectron current from the satellite (I_{ph}). The satellite surface potential ϕ_s at any point P defined by the angles θ and ϕ is

$$\phi_s = \phi_{eq} - VBR\cos\theta \tag{1}$$

where ϕ_{eq} is the potential on the equatorial plane of the satellite. It is assumed[1] that 1) the thermal velocities of ions ($\bar{v}_i$) and electrons ($\bar{v}_e$), and the satellite speed are such that $\bar{v}_i \ll V \ll \bar{v}_e$; 2) the ions are uninfluenced by the magnetic field whereas the electrons may be considered moving with thermal velocity relative to the satellite along B lines. The electron current density J_e to the satellite at the point P is[1]

$$J_e = n_0 e\left(\frac{kT}{2\pi m_e}\right)^{1/2} \exp\left(\epsilon\frac{e\phi_s}{kT}\right)\sin\theta\cos\phi, \quad -\tfrac{1}{2}\pi \le \phi \le \tfrac{1}{2}\pi \tag{2}$$

Received May 27, 1980; revision received October 10, 1980.

*Associate Researcher, on leave from India Span Research Organization, Trivandrum, India. Member AIAA.

where n_0, T, m_e, e, and k are the number density of electrons or ions, electron or ion temperature, electron mass, electron charge, and the Boltzmann constant, respectively. $\epsilon = 1$ if $\phi_s < 0$ and $\epsilon = 0$ if $\phi_s \ge 0$. Wake structure studies[5,6] indicate that because of the depletion of ions, there is a potential barrier in the wake shielding the downstream surface of the satellite from the electrons. Here the electrons are moving in a direction perpendicular to satellite velocity. The self-consistent three-dimensional numerical solution for this case done in Ref. 6 indicates that barrier potentials are predominant in the region, 225 deg $< \phi <$ 315 deg. Thus to account for the potential barrier for electrons, Eq. (2) is integrated on ϕ from $-\frac{1}{4}\pi$ to $\frac{1}{2}\pi$. Integrating Eq. (2) and considering the electron flux in both directions along B, the electron current is

$$I_e = 2n_0 eR^2\left(\frac{kT}{2\pi m_e}\right)^{1/2}\left[K\exp\left(\frac{e\phi_{eq}}{kT}\right) \times \int_0^{\theta'} \exp(-\alpha\cos\theta)\sin^2\theta\, d\theta + \left(\pi - \theta' + \frac{\sin 2\theta'}{2}\right)\right] \tag{3}$$

where θ' is the value of θ at which ϕ_s changes from negative to positive potential and $\alpha = eBRV/(kT)$ is the nondimensional induced potential. K is a factor depending on the range of integration of ϕ (here $K = 1.707$). If the assumption of neglecting the ion thermal velocity and treating them as neutral particles is made,[1,2] the ion current density at P is

$$J_i = n_0 eV\sin\theta\sin\phi, \quad 0 \le \theta, \quad \phi \le \pi \tag{4}$$

The assumption of ion thermal motion being negligible compared to satellite velocity is an increasingly poor approximation with increasing altitudes,[2] and following Ref. 2, the ion thermal motion can be taken into account by including the average ion velocity. Thus, the ion current density becomes

$$J_i = n_0 e[V^2 + 8kT/(\pi m_i)]^{1/2}\sin\theta\sin\phi \tag{5}$$

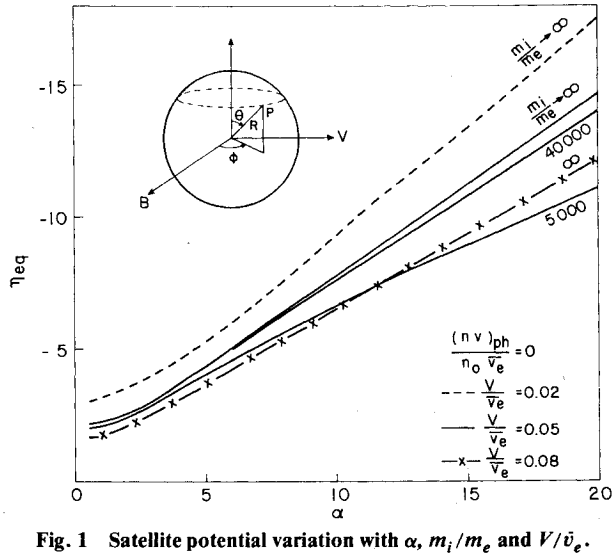

Fig. 1 Satellite potential variation with α, m_i/m_e and $V/\bar{v}_e$.

where m_i is the ion mass. Chang and Smith[7] have considered the effect of attraction of ions in a spherically symmetric field, by a constant potential satellite, by defining an increased radius $R(1-e\phi_s/E_i)^{1/2}$, where E_i is the ion kinetic energy. Here the expression of Ref. 7 is used by replacing ϕ_s, by the average potential, that is by $\phi_{eq}-VBR\sin\theta'/\theta'$ for $0<\theta<\theta'$ and by $\phi_{eq}+VBR\sin\theta'/(\pi-\theta')$ for $\theta'<\theta<\pi$. Thus, the ion current to the satellite can be written as

$$I_i=n_0eR^2\left(V^2+\frac{8kT}{\pi m_i}\right)^{1/2}\int_0^{\pi}\left(\int_0^{\theta'}1-\frac{e(\phi_{eq}-VBR\sin\theta'/\theta')}{\frac{1}{2}m_i(V^2+8kT/\pi m_i)}\right.$$
$$\left.+\int_{\theta'}^{\pi}1-\frac{e[\phi_{eq}+VBR\sin\theta'/(\pi-\theta')]}{\frac{1}{2}m_i(V^2+8kT/\pi m_i)}\right)\sin^2\theta\,d\theta\sin\phi\,d\phi \quad (6)$$

which integrates to

$$I_i=n_0eR^2\left(V^2+\frac{8kT_i}{\pi m_i}\right)^{1/2}\left[\left(1-\frac{e(\phi_{eq}-VBR\sin\theta'/\theta')}{\frac{1}{2}m_i(V^2+8kT/\pi m_i)}\right)\right.$$
$$\times\left(\theta'-\frac{\sin2\theta'}{2}\right)+\left(1-\frac{e[\phi_{eq}+VBR\sin\theta'/(\pi-\theta')]}{\frac{1}{2}m_i(V^2+8kT/\pi m_i)}\right)$$
$$\left.\times\left(\pi-\theta'+\frac{\sin2\theta'}{2}\right)\right] \quad (7)$$

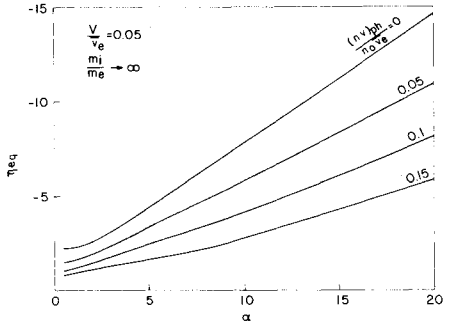

Fig. 2 Satellite potential variation with α and $(nv)_{ph}/(n_0\bar{v}_e)$.

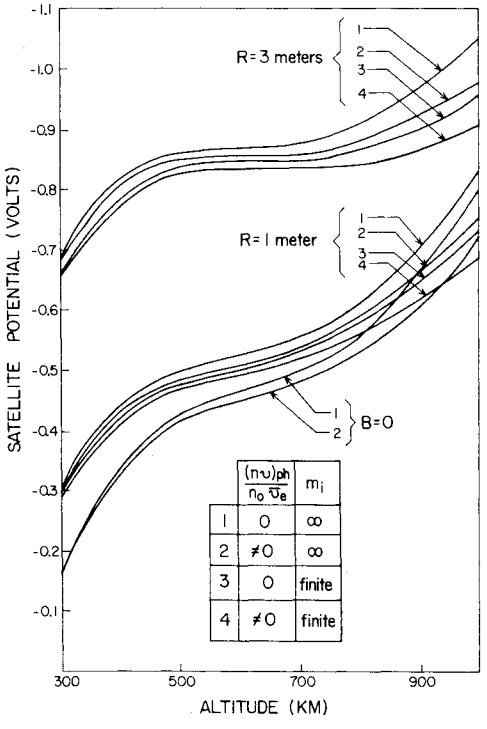

Fig. 3 Potential variation with altitude.

The photoelectric current I_{ph} can be written (after cutting off the contribution from the positive region at $\theta=\theta^P$, where θ^P is the angle at which the potential is 1 V) as[1]

$$I_{ph}=(nv)_{ph}eR^2(\theta^P-\tfrac{1}{2}\sin2\theta^P) \quad (8)$$

where $(nv)_{ph}$ is the photoelectron flux from unit area per second (about 3×10^{14} particles per square meter). The satellite surface potential is obtained from the condition

$$I_e=I_i+I_{ph} \quad (9)$$

In view of the large number of ionospheric parameters involved and the variation of these parameters due to solar activity, summer and winter, day and night, it is worthwhile to nondimensionalize Eq. (9) in terms of the following nondimensional quantities:

Nondimensional satellite potential $\eta_{eq}=e\phi_{eq}/(kT)$; ratio of satellite velocity to average electron velocity $=V/\bar{v}_e$; ratio of photoelectron flux to electron flux $=(nv)_{ph}/(n_0\bar{v}_e)$; ratio ion mass to electron mass $=m_i/m_e$. Substituting Eqs. (3), (7), and (8) in Eq. (9), the nondimensional satellite potential is

$$\exp(\eta_{eq})=\left\{2\left(\frac{V^2}{\bar{v}_e^2}+\frac{m_e}{m_i}\right)^{1/2}\left[\left(\theta'-\frac{\sin2\theta'}{2}\right)\right.\right.$$
$$\times\left(1-\frac{\pi(\eta_{eq}-\alpha\sin\theta'/\theta')}{4(m_i/m_e)(V^2/\bar{v}_e^2+m_e/m_i)}\right)+\left(\pi-\theta'+\frac{\sin2\theta'}{2}\right)$$
$$\left.\times\left(1-\frac{\pi[\eta_{eq}+\alpha\sin\theta'/(\pi-\theta')]}{4(m_i/m_e)(V^2/\bar{v}_e^2+m_e/m_i)}\right)\right]+\frac{2(nv)_{ph}}{n_0\bar{v}_e}$$
$$\left.\times\left(\theta^P-\frac{\sin2\theta^P}{2}\right)-\left(\pi-\theta'+\frac{\sin2\theta'}{2}\right)\right\}$$
$$\times\left(K\int_0^{\theta'}\sin^2\theta\exp(-\alpha\cos\theta)\,d\theta\right)^{-1} \quad (10)$$

and

$$\eta_{eq}-\alpha\cos\theta'=0 \quad (11)$$

If the satellite is negative everywhere, Eq. (10) reduces to

$$\exp\eta_{eq}=\frac{2\alpha}{KI_1(\alpha)}\left[\left(\frac{V^2}{\bar{v}_e^2}+\frac{m_e}{m_i}\right)^{1/2}\right.$$
$$\left.\times\left(1-\frac{\pi\eta_{eq}}{4(m_i/m_e)(V^2/\bar{v}_e^2+m_e/m_i)}\right)+\frac{(nv)_{ph}}{n_0\bar{v}_e}\right] \quad (12)$$

where $I_1(\alpha)$ is the modified Bessel function of the first kind. When the magnetic field and ion thermal motion are neglected and $K=2$, Eq. (12) reduces to the result of Ref. 2.

Results and Discussions

Equations (10) and (11) have been solved numerically and the results are presented in Figs. 1 and 2, where η_{eq} is plotted against α with $V/\bar{v}_e$, m_i/m_e, and $(nv)_{ph}/n_0\bar{v}_e$ as parameters. Calculations have also been made for spherical satellites of 1 and 3 m diam using the ionospheric properties of Ref. 8, and the results are shown in Fig. 3. It is seen from Fig. 1 that for $\alpha>5$, η_{eq} varies almost linearly with α. For low α (small satellites) Fig. 1 shows that the ion thermal motion has negligible influence on η_{eq}, but for high α, low values of m_i/m_e can increase η_{eq} by 20%. It is also seen from Figs. 1 and 2 that a 50% increase in $V/\bar{v}_e$ or $(nv)_{ph}/(n_0\bar{v}_e)$ increases η_{eq} by about 20% for all α. Figure 3 shows that for a given satellite, the effect of ion thermal motion and photoelectric effect are small at low altitude (<600 km), but increase with altitude. For example, at 1000 km, for a 3-m-diam satellite, the photoelectric effect can increase the satellite potential by

7% and ion thermal motion by 8%. Thus, the effect of ion thermal motion and photoelectric effect on satellite potential are of the same order.

References

[1]Hohl, F., "The Electromagnetic Torques on Spherical Earth Satellites in a Rarefied Partially Ionized Atmosphere," NASA TR R-231, Feb. 1966.

[2]Kasha, M.E., "The Ionosphere and its Interaction with Satellites," Gordon and Breach, New York, 1969, pp. 47-73.

[3]Pike, C.P. and Lovell, R.R., *Proceedings of the Spacecraft Charging Technology Conference,* NASA TMX-73537, Feb. 1977.

[4]Rosen, A., "Spacecraft Charging: Environment-Induced Anomalies," *Journal of Spaceraft and Rockets,* Vol. 13, March 1976, pp. 129-163.

[5]Samir, U., Gordon, R., Brace, L. and Theis, R., "The Near-Wake Structure of the Atmosphere Explorer C (AE-C) Satellite: A Parametric Investigation," *Journal of the Geophysical Research,* Vol. 84 (A2), Feb. 1979, pp. 513-525.

[6]Shea, J.J., "Collisionless Plasma Flow Around a Conducting Sphere in a Magnetic Field," *Rarefied Gas Dynamics,* Supplement 4, Vol. II, Academic Press, New York, 1967, pp. 1671-1686.

[7]Chang, H.H.C. and Smith, M.C., "On the Drag of a Spherical Satellite Moving in a Partially Ionized Atmosphere," *Journal of the British Interplanetary Society,* Vol. 17, Jan.-Feb. 1960, pp. 199-205.

[8]deLeeuw, J.H., "A Brief Introduction to Ionospheric Aerodynamics," *Rarefied Gas Dynamics,* Supplement 4, Vol. II, Academic Press, New York, 1967, p. 1564.

AIAA 80-0808R

Computerized Process for Calculation of Discrete Test Loads

H. A. Tutty* and R.S. Lahey†
Lockheed, Burbank, Calif.

Introduction

A STRUCTURAL test is a process of imposing applicably distributed loads to a structure and recording the structure response. Most activities associated with testing evolve around the subject of loads – what type, how much, when, and where. The success of a structural test is contingent on the timely, accurate determination of the test loads data.

An extensive structural test program of a full-scale production Space Shuttle Orbiter was recently completed. This program was conducted to supplement and validate the stress analysis and to demonstrate the structural integrity of the vehicle when subjected to design loads.

This multifaceted test program was initiated in 1974 and was completed in late 1979. A total of 388 hydraulic actuators (jacks), strategically located over the external airframe surface were required to apply the design loads. In addition, over 5000 sensors (strain gages, deflectometers, load transducers, and thermocouples) were used to measure the structure's response. Closed loop servo systems were controlled by computers to apply precise synchronous loading of the jacks.

The test article, which is the scheduled second flight vehicle, consisted of a structurally complete full-scale orbiter less certain items of functional hardware, such as landing gears, crew module, and control surface actuators. Substitute hardware was designed and fabricated for these missing items as well as substitute payload which distributed applied loads into test.

The Test Program encompassed four sequences: influence coefficient tests; 120% limit load tests; aft fuselage pressure test; and forward fuselage thermal test.

The second sequence and major portion of the test program was the limit-load testing. A total of 38 loading applications were imposed on the airframe to simulate the critical design conditions in the launch, re-entry, and landing modes. The number of test conditions and complexity of the test setup required the implementation of a discrete test-loads computer program.

Structural Test Requirements

The computerized technique of deriving discrete test-loads began simultaneously in two areas. One area was the development of an acceptable test-load matrix. The second area was the development of the loading systems concepts.

The test-load matrix originated from the vehicle stress analysis load description. The stress-load description was presented in a 21,500 node point matrix. Each node point had three degrees of freedom; shear, x, y, and z, for a total of 64,500 degrees of freedom. This matrix was much too large and detailed a comprehensive loads input for a static structural test. To provide an applicable load description, the loads from this matrix were operated on by transform equations to provide the fixed test-grid matrix of 836 node points and 2,400 degrees of freedom.

The next step was to consolidate all of the 38 test-loading applications. These data, plus the test node grid geometry, the position of the movable surfaces, and a brief description of the loading application were recorded on a magnetic tape. This tape was then made accessible to both the main jack loads program and the interactive fixture design and verification programs.

The loading system concepts for most substructures were evaluated and refined using interactive computer programs which directly access the external test-load data. The development of acceptable loading concepts is an iterative process. A preliminary concept is first established and then analyzed for the critical design loads. The loading concept is then refined and the process is repeated. The results of each iteration is used to modify or validate the concept. The evaluation of these concepts was a coordinated effort involving the vehicle structural analysis and test organizations.

Program Description

The discrete jack loads program provides mechanisms to use the detailed knowledge of local conditions, while matching the gross external load distributions and maintaining test load within the mechanical capability of the test equipment.

The jack-loads program required, in addition to the external test-load matrix, three data sets: jack, ratio, and group.

The jack data set is the definition of the test geometry. This data set includes: jack and static test support locations; jack and static test support orientation; jack train definition; and jack piston areas.

A ratio is defined as a group of jacks which are loaded in a constant relationship designed to produce a required load vector. Ratios are developed and used in conjunction with specific jacks to produce a desired loading effect. The ratio data set includes: location; vector identification; jack orientation; and jack weightings.

The group data set is a model of the loading system over a specific portion of a structure. The group data set defines the relationship of jacks and ratios to the individual degrees of freedom of the test-loads matrix. In a given group, specific jacks and ratios are used to satisfy the shears and moments developed by unit loads in the degrees of freedom (DOF)

Presented as Paper 80-0808 at the AIAA/ASME/ASCE/AHS 21st Structures, Structural Dynamics & Materials Conference, Seattle, Wash., May 12-14, 1980; received July 10, 1980; revision received Nov. 15, 1980.

*Research Specialist, Structures & Materials Laboratory.
†Design Specialist, Advanced Structures Technology.